

Estimation of Layered Ink Layout from Arbitrary Skin Color and Translucency in Inkjet 3D Printer

Junki Yoshii ¹⁾, Shoji Yamamoto ²⁾, Kazuki Nagasawa ¹⁾, Wataru Arai ³⁾, Satoshi Kaneko ³⁾, Keita Hirai ¹⁾, Norimichi Tsumura ¹⁾

1) Graduate School of Science and Engineering, Chiba University, CHIBA, JAPAN

2) Tokyo Metropolitan College of Industrial Technology, TOKYO, JAPAN

3) MIMAKI ENGINEERING Corporation, NAGANO, JAPAN

Abstract

In this paper, we propose a layout estimation method for multi-layered ink by using PSF measurement and machine learning. This estimation can bring various capabilities of color reproduction for the newfangled 3D printer that can apply multi-layered inkjet color. Especially, the control of translucency is useful for the reproduction of skin color that is overpainted flesh color on bloody-red layer. Conventional method of this layer design and color selection depended on the experience of professional designer. However, it is difficult to optimize the color selection and layer design for reproducing complex colors with many layers. Therefore, in this research, we developed an efficiency estimation of color layout for human skin with arbitrary translucency by using machine learning. Our proposed method employs PSF measurement for quantifying the color translucency of overlapped layers. The machine learning was performed by using the correspondence between these measured PSFs and multi-layered printings with 5-layer neural network. The result was evaluated in the CG simulation with the combination of 14 colors and 10 layers. The result shows that our proposed method can derive an appropriate combination which reproduce the appearance close to the target color and translucency.

1. Introduction

In recent years, 3D printers are widely used for the design assessment and rapid proto-typing in the industrial field. Various modeling type of 3D printers exist such as fused filament, stereolithography, selective laser sintering, and inkjet method. The most accurate type is stereolithography modeling, and is used in the medical field such as medical [1] and dental [2], although there are some limitations for printing material. A part of automobiles [3] and consumer concept model are recently made by inkjet type 3D printer with fine jetting. This inkjet type has unique and superior feature which can make colored product. Furthermore, by combining with various surface fabrication, other applications such as welfare device and architectural models are expected in the foreseeable future.

For the faithful reproduction as an industrial application, it is important to equip the expressive ability of appearance including the color, surface reflectance, and translucency. Since recent printer has a polisher and clear coat layer, inkjet 3D printer is possible to reproduce various behavior of surface reflection with glossiness. Also, the expression of translucency is possible to reproduce by using a stack of thin layers. For example, the skin of Japanese humanoid doll is realized by combining beige and red layer for real shading by muscled body. This attempt of translucency in stomach muscles provides dynamic volume and vivacious appearance as a realistic human body. The application of translucency is essential to the formation of a natural object, although the disadvantage is long manufacturing time by reason of the thin layers.

In addition, there are other difficulties of how to choose the color of many layers and how to decide their order for the realization of translucency. In general, the translucency and degree of dispersion depend on materials of inkjet 3D printer. With a few layers, it is possible to estimate the result of reproduction. Professional designer may be possible to decide an appropriate combination of color layers based on their experiences. However, it is quite difficult to determine the combination of layers that achieve the desired color and degree of dispersion at the case of multiple layers.

Therefore, in this research, we propose an estimation method to find an appropriate combination of multiple layers which can realize the modeling with desired color and translucency. Fig. 1 shows the outline of proposed method. At first, the target color and translucency are derived from the rendering engine based on the designer's concept. In the estimation process, we employ the machine learning with neural network. This network can calculate the best selection of layer structure relative to the desired color and translucency as inputs of this network. Here, it is noted that some limitations exist in this research; target object consists only of human skin with multi-layer and the characteristic of translucency is prioritized against other appearance such as color and surface reflectance.

Designer shape the Multi-layered Objects (Human Skin) with Material Appearance by 3D Printer.

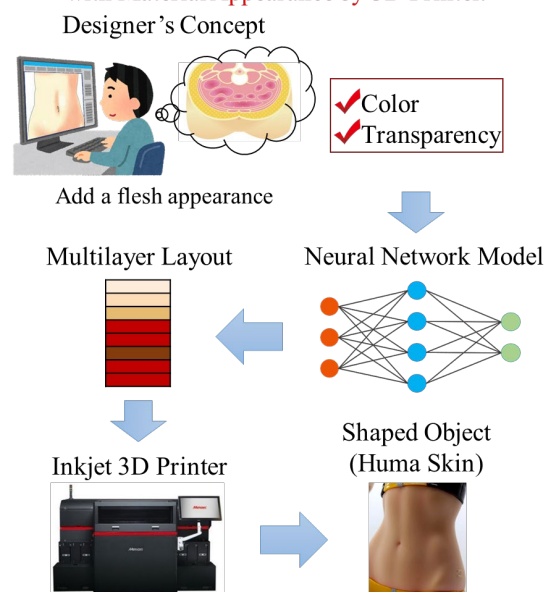


Figure 1. The outline of this research

2. Related Works

A color reproduction in 3D inkjet printer have been developed by using different approach compared with 2D inkjet printer. A same printing method such as halftone often generated some artifacts since the generated dot in 3D printer was bigger than the dot in 2D printer. In order to decrease these artifacts, Brunton et al. proposed a novel traversal algorithm for voxel surfaces as shown in Fig.2 [4]. Their challenge accomplished faithfully color reproduction, color gradients and fine-scale details. Unfortunately, it has disaffection to completely solve the loss of image contrast due to overpainting.

Instead of halftoning, Babael et al. used the contoning method to realize a wide color gamut [5]. This method should consider the combination of inks with various thicknesses inside the object's volume. Therefore, they proposed color prediction model based on the Kubelka-Munk absorption. Although it was hard to reproduce perfect color matching only with a few layer of CMYK inks, the possibility for fine reproduction in 3D inkjet printer exists by using the contoning with multiple ink layers. Moreover, their contribution in this research also made us realize the importance of controlling image blurring and translucency of color due to layer overlap.

As the measurement-based method, Shi et al. tried to reproduce faithfully color matching by using multi-spectral imaging and machine learning techniques as shown in Fig.3 [6]. In this research, they use two neural networks to learn the color reproduction with combination of layers and the gamut range by multiple layer, adversarially. First, they obtained spectral reflectance for 20878 patches, and learn a network (F) to associate them with their layout. Using this model, the layout prediction model (B) was trained in order to minimize the errors of loss functions with respect to the output spectrum. Here, E_{spec} is an error function that minimizes the difference between the spectrum of the sample (painting) and F. E_{LAB} is an optimization function that express LAB color space between the spectrum of the sample and the spectrum from F. Finally, E_{thick} is a function that minimizes the thickness of the color layer. This function is necessary for inhabitation of the thickness in color layer and increase of dot gains. They use the sum of the above three loss functions as the total loss function of model B.

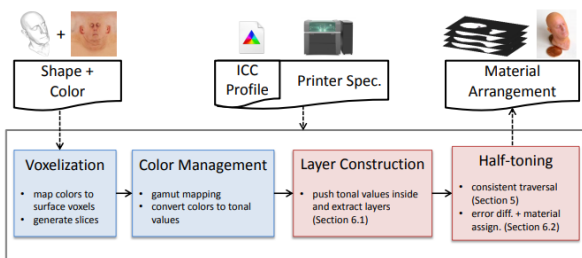


Figure 2. Flow-chart of processing pipeline by A. Brunton, et al., [4]

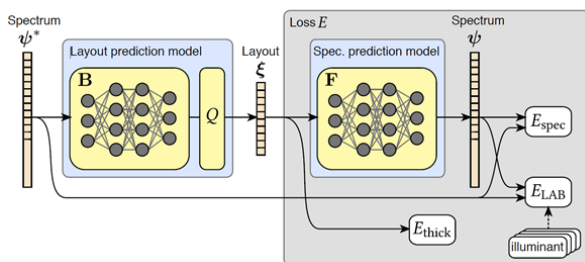


Figure 3. Illustration of our network structure by L. Shi, et al., [6]

Their proposed method indicates a state-of-art color matching even if the number of colored layer increases. However, we think that it is necessary to consider the image blur with translucency if the characteristic of dispersion is different each color layer. Especially, in the reproduction of human skin, it is very important to control the translucency in the stack of layer. Therefore, in our research, we focus on the control of translucency by using the measurement and machine learning method.

3. Definition of Color Patch for Human Skin

At first, we defined color patches of human skin with arbitrary translucency for the estimation of appropriate layers in a 3D printer. Human skin has a typical multi-layered structure because the relationship of each layer is roughly determined. The biological model of skin was well-known in the research field of measurement and simulation [7] However, in the case of 3D printer, it is difficult to apply this model directly, since color information is redundant. Therefore, in this research, we assume that the multilayer structure of human skin is approximated using three types of clear layer, epidermal layer and dermal layer.

Next, we selected the color which is assigned to each of the three approximate layers. The clear layer is greatly used as the control factor for the translucency of human skin. The epidermal layer (epidermis) represents a flesh colored layer located as the cover of the skin, and the dermal layer (dermis) represents a red layer in which human blood is flowing. Here, we should define the color information of each layer with combination of CMYK colors. In this case, we selected three colors empirically as follows; the flesh color represents typical Asian color of skin, and arbitrary red 10 color is selected for dermis layer. The clear layer is only one type represented as the combination of all zero in CMYK. Moreover, we should decide the total number of layers in order to reproduce the skin appearance in 3D printer. In this research, the total number of ink layers is fixed as 10 layers because the mixed color with more than 10 layers are superimposed, and it may become black due to subtractive color effect. The order of the clear layer, the epidermal layer and the dermal layer is fixed as shown in Fig. 4.

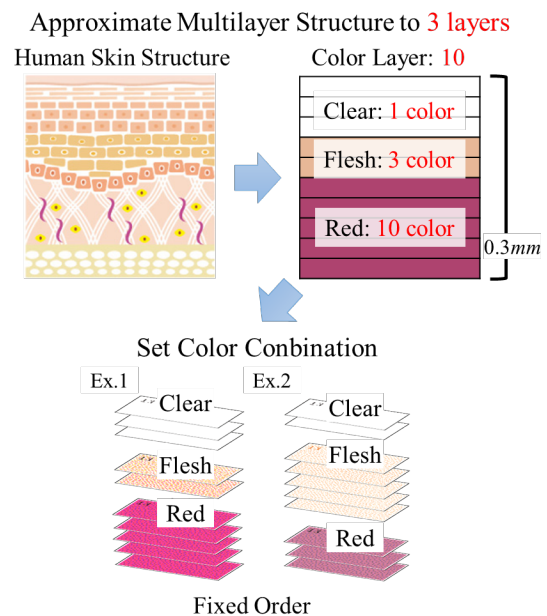


Figure 4. Conditions for shaping human skin color patches

As the final step, we make the test color patches for the simulation of skin color and translucency. Each color patch size is 1 cm square, and the total number of combined patches is 1875. Here, in this case, the total number of color combinations become 30 which consist of 1 clear color, 3 flesh color and 10 red colors ($= 1 \times 3 \times 10$). Also, the total number of combined layers become 66 with 10 color layers ($= {}_{12}C_2$). Therefore, all patterns become 1980 ($= 30 \times 66$). However, we reduced the total number to 1850 with equal decimation, since our 3D printer only make three plates with 625 patches at one time.

Otherwise than previous condition, an opaque white margin is placed between each patch to prevent the ink on each patch from bleeding and the incident light on any patch from entering the next patch. In addition, white ink is placed on the back of each patch in order to prevent transmission of incident light and to prevent the printed plate from bending.

4. Calculation Method of LSF

The setting condition and each relationship of measuring devices are shown in Fig. 5. In this study, we measured LSF (Linear Spread Function) and calculated as an index of translucency in the reproduction of human skin [8]. A laser projector (Smart Beam Laser, United Object) was used as the illuminator that emits a line toward each patch. This projector has 1280×720 resolution, and each pixel is possible to control by Liquid Crystal on Silicon (LCOS). The projected image is

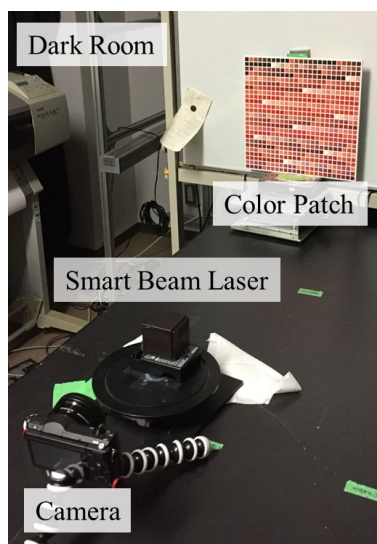


Figure 5. Condition for imaging the color patch

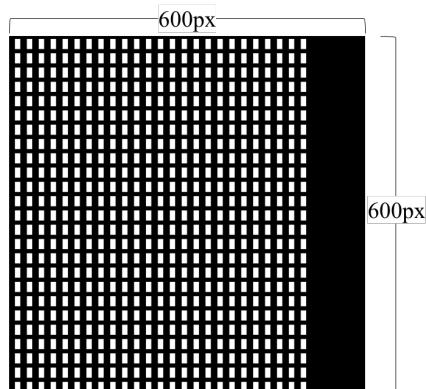


Figure 6. Input image to projector for projecting light pattern on the patch

shown in Fig. 6 for irradiating half of the patch in order to obtain the characteristic of LSF. High-resolution camera ($\alpha 5100$, SONY) was used as a captured device which had 6000×4000 resolution. We set the shutter speed to 1 second, and the ISO sets to 100. Since the size of the plate is 30 cm with 1 cm patches, this camera has enough resolution to measure the LSF of each patch.

An example of a projected color patch is shown in Fig. 7. Since many color patches exist for each color, it is necessary to automate each LSF calculation for the purpose of efficiency. At first, the left half of patch is illuminated as shown in Fig. 8 (a). Therefore, we obtain the change in pixel value from the left to the right in the middle of the patch in order to measure the degree of light blur. The obtained results are shown in Fig. 8 (b). At next time, some transitions of the pixel value are acquired in the same way in the patch since noise is included in the acquired pixel values. Here, it is noted that the noise is removed by averaging them. Figure 8 (c) shows the result of differentiating the transition of the pixel value. The LSF is divided into RGB to obtain patch color information. However, the degree of light blur assumes isotropic and evenness when we acquire the LSF. Therefore, only the front side (the left side in the color patch) is used as an assumption of isotropy since the transition is different

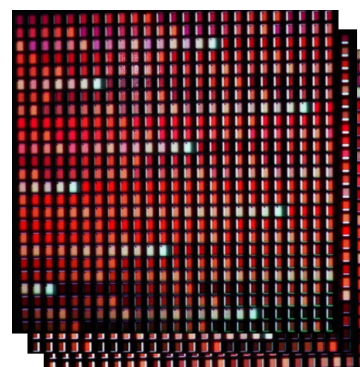


Figure 7. Color patches illuminated half by the laser projector

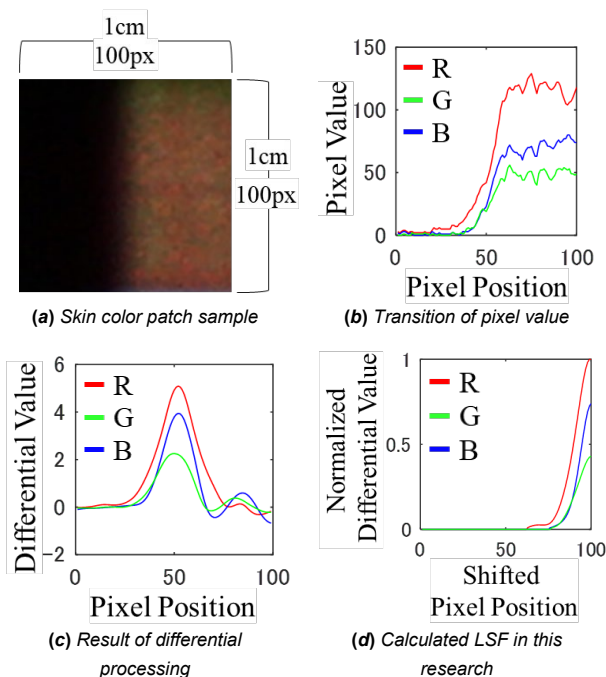


Figure 8. Processing flow for LSF acquisition

before and after the peak of the differential value. After smoothing to remove the noise of the differential value, the data less than 0 is corrected to 0 as an error. The LSF obtained through the above process is shown in Fig. 8 (d). The same process is applied to all 1875 skin patches.

5. Training of Neural Network Model

Next, we train a neural network to associate the LSF data for the 1875 skin patches with the layouts representing the color assignment to each layer in the corresponding patch. It is possible to predict the layout of human skin patches with arbitrary translucency by this learning result. In the total 1875 data sets, 1500 training data and 375 test data are set separately. The training and the test sets are randomly extracted from the data sets. Here, the value of LSF contains RGB information. Therefore, an input array of LSF values become 300 (3×100) data in RGB order. The output layout values are expressed by assigning numbers to each 14 colors, which are combination of clear, flesh color and red in total. And the number to each layer becomes 10 as an output layers. Here, the number of clear color is indicated as 1, flesh 3 colors representing the epidermis layer are indicated as 2 to 4, and red color in 10 colors representing the dermal layer are indicated as 5 to 14.

In our neural network, each neuron is completely connected and the hidden layer is composed of four stages. All hidden layers consist of 32 neurons with the ReLU activation function. The number of neurons is determined to minimize the error in the test set. The loss function employs the mean squared error and the loss is calculated using the previously trained inverse model. The model is trained by the stochastic optimization algorithm: Adam. The initial learning rate is set to 10^{-3} , and the batch size and the number of epochs are set to 25 and 1000, respectively. The structure of this neural network is shown in Fig. 9. We use the structure and the setting of Liang Shi et al. (2018) [6] as reference.

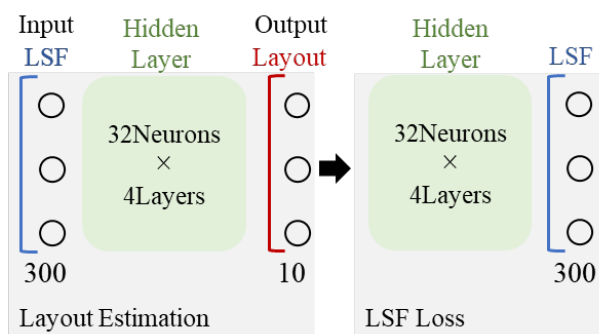
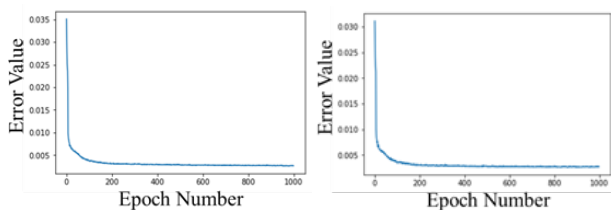


Figure 9. Structure of the neural network



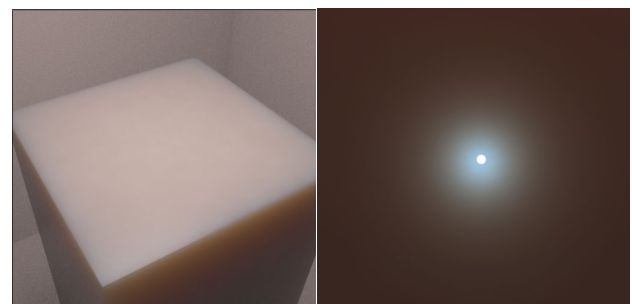
(a) Error in the training set (b) Error in the test set

Figure 10. Transition of the error by the mean square

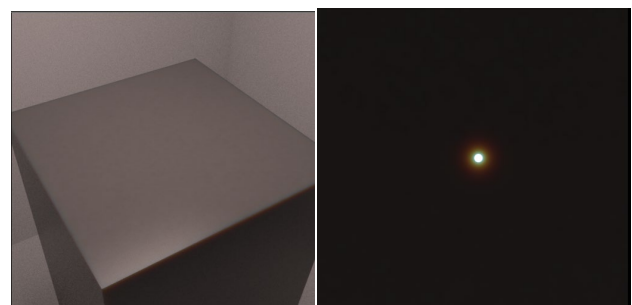
As a learning result of the constructed neural network, Fig. 10 (a) shows the value of the error in the training set calculated by the mean square error function for each epoch. The mean squared error function is performed on the LSF value estimated by the last layer of our neural network and the LSF value at the input layer. From the result in Fig. 10 (a), we found that the error has already converged to 0 at around 300 epochs. The minimum value of the error becomes 0.002672 as small as possible. As shown in Fig. 10 (b), the minimum value of the error becomes 0.002697 in the loss function for test set.

6. Evaluation of skin with rendering result

The layout can be predicted when the designer renders human skin on CG by the learned neural network. Therefore, we evaluate the result of machine learning by reproducing the CG of human skin with expected translucency. In order to control the color and the translucency of translucent objects such as human skin, it is necessary to specify the absorption coefficient and the scattering coefficient of the object. Therefore, we use the general material appearance of Asian skin as an example of human skin [9]. First, the typical RGB value (700.00, 546.10, 435.80 nm) are used as the wavelength of monochromatic light of RGB specified by CIE. Next, we calculate the absorption coefficient of black-brown Eumelanin contained in human skin and the absorption coefficient of orange-brown Pheomelanin, where the content ratio of the Eumelanin is set to 0.7. Next, we calculate the absorption coefficient in the area without melanin. We set the content ratio of melanin containing the Eumelanin and the Pheomelanin in the skin to 0.12. These values are all Asian averages. We use these values to calculate the absorption coefficient and the isotropic scattering coefficient of the human skin. The result of calculated absorption coefficient is indicated as (R, G, B) = (2.2035, 5.3338, 12.178), and the isotropic



(a) Standard human skin (b) PSF obtained by (a)



(c) Human skin with modulated translucency (d) PSF obtained by (c)

Figure 11. Reproduction of human skin by CG and its PSF

scattering coefficients are indicated as (R, G, B) = (191, 28, 381.59, 774.31). The rendering result of cube with above coefficients is shown in Fig. 11 (a). Figure 11 (b) shows an enlarged view of the standard human skin with the spot light applied. Based on this image, we calculate the LSF used as the input of the neural network learned in the previous section. In order to manipulate the translucency of the rendered human skin, the obtained absorption coefficient is empirically multiplied by a constant in this study. We obtained the rendering results as shown in Fig. 11 (c) by multiplying the absorption coefficient of the standard human skin by 100. The resulting image is shown in Fig. 11 (d) with a spot light applied to it. It can be seen that the spread of the laser beam is different in comparison to Fig. 11 (b).

7. Layout Prediction by Machine Learning

The LSF of the rendered human skin is acquired and input to the learned neural network to predict its layout. We calculate LSF based on the PSF (Point Spread Function) of the image where the narrow spot light is projected on CG human skin. LSF makes each RGB component have 100 values in a total of 300 arrays as well as the learned setting. We used Mitsuba^[10] for rendering. The obtained LSF is input to the learned network and we show the layout result estimated by it in the Fig. 12 (a). This figure shows the estimated color numbers for each layer, and the corresponding color patch was placed under the color number. In this method, we fix the order of the color layer consisting of the clear layer, the flesh color layer and the red layer, and the final output value is generated by assigning just one color number to each color layer. Therefore, this output result needs to be corrected to match this setting. The color numbers assigned to each color layer are determined by averaging the estimated color numbers. Averaging is performed on the color numbers for each color layer. In the example of Fig. 12 (a), the flesh color layer continues from layer number 1 to 6, and

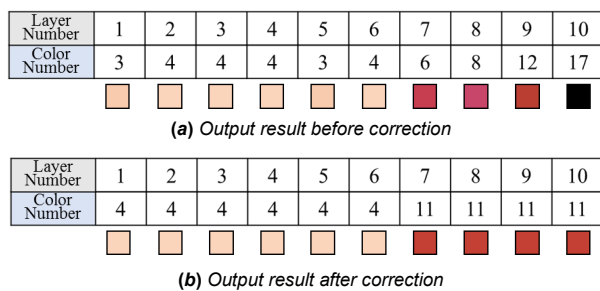


Figure 12. Output result by the neural network model in this research

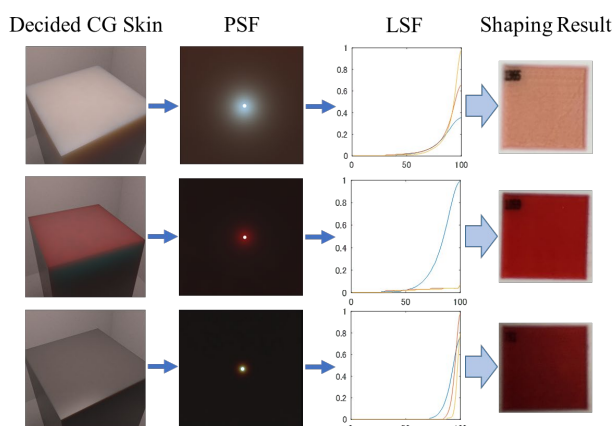


Figure 13. Layout prediction result of CG skin using neural network

the red layer continues from layer number 6 to 12. When the number of layers is 10, it is shown in black because the number of colors not set in this study is estimated. However, we average the output values including these outliers in each color layer. As a result, the color numbers are as shown in Fig. 12 (b). Fig. 13 shows the flow from inputting LSF of rendered CG human skin to a learned neural network and outputting a color patch with an estimated layout. In almost cases, it was possible to estimate the faithful result similar to the appearance of the human skin reproduced by CG. However, as for the lower brownish human skin, the estimation result was slightly reddish.

In order to confirm the validity of the estimation results, we select the sample with the LSF with the smallest mean difference value from the LSF of human skin created by CG. Figure 14 shows target CG human skin and its LSF, and selected LSF with the closest shape to this LSF of CG skin patch with the value of the mean error. In the shaped samples, it can be seen that there are other patches with LSF closer to the target LSF than the LSF estimated by this network model. The main reason is that there is no patch in the shaped samples with an LSF that matches the LSF of CG human skin. The layout values (Fig. 12 (b)) were set to be output according to the layout of the already shaped samples without directly shaping the layouts predicted in this network. Therefore, the LSF of CG human skin and the LSF of patch are hard to match with some differences. In addition, the colors were slightly different even though these LSF were similar. From this result, it is obvious that we need to reconsider the LSF calculation and color selection method with consideration for the balance of color and LSF information.

8. Conclusion and Future works

In this research, we proposed an estimation method to select the best multiple layers of human skin with arbitrary translucency for the application of inkjet 3D printer. Various combination of LSF information for translucency were measured, and an appropriate layout of multiple layers was derived from the result of machine learning.

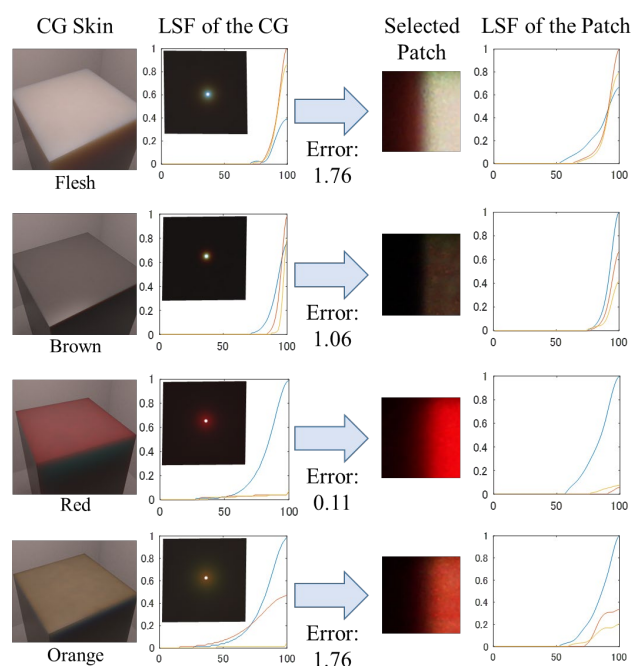


Figure 14. Search result of LSF closest to the LSF of CG skin

As a preliminary study, we focused on the LSF matching with the limitation of the application for human skin. Therefore, it is possible to select a combination of layers that produces very similar LSFs as the result of estimation, despite the complexity of 10 layers. On the other hand, unfortunately, it is hard to find the best combination that satisfies both color and LSF. We believe that an accurate estimation requires more learning samples and complex networks.

Moreover, we imposed the restrictions of overpainting in each part such as clear, epidermis, and the dermis. However, we never make the restriction for the learning process. We assume that it is necessary to separate networks by features such as BSSRDF^[11] and LSF to avoid complicated learning, and comprehensive error propagation must be considered.

Acknowledgement

This research was partially supported by JSPS KAKENHI Grant Number 17K00266 and 18K11540.

References

- [1] C. L. Ventola, "Medical Applications for 3D Printing: Current and Projected Uses", *P&T*, Vol.39, No.10, pp.704-711, 2014.
- [2] A. Dawood, B. Marti, V. Sauret-Jackson & A. Darwood, "3D printing in dentistry", *British dental journal*, Vol. 219, pp.521-529, 2015.
- [3] X. Wang, Q. Guo, X. Cai, S. Zhou, B. Kobe, and J. Yang, "Initiator-Integrated 3D Printing Enables the Formation of Complex Metallic Architectures", *ACS Appl. Mater. Interfaces*, 6 (4), pp 2583-2587, 2014.
- [4] A. Brunton, C. A. Arikian, P. Urban, "Pushing the Limits of 3D Color Printing: Error Diffusion with Translucent Materials", *ACM Trans. Graph.*, 35(1), article No.4, 2015.
- [5] V. Babaei, K. Vidimčec, M. Foshey, A. Kaspar, P. Didyk, and W. Matusik, "Color contouring for 3D printing", *ACM Trans. Graph.* (SIGGRAPH), 36(4), pp.1-15, 2017.
- [6] L. Shi, V. Babaei, C. Kim, M. Foshey, Y. Hu, P. Sitthi-Amorn, S. Rusinkiewicz, W. Matusik, "Deep Multispectral Painting Reproduction via Multi-Layer, Custom-Ink Printing", *ACM Transactions on Graphics*, Vol. 37, No. 6, 2018.
- [7] I. V. Meglinsky, S. J. Matcher, "Modelling the sampling volume for skin blood oxygenation measurements", *Medical and Biological Engineering and Computing*, Vol. 39, Issue 1, pp 44-50, (2001).
- [8] K. Happel, M. Walter, E. Dörsam, "Measuring Anisotropic Light Scatter within Graphic Arts Papers for Modeling Optical Dot Gain", *18th Color and Imaging Conference*, pp.347-352, 2010.
- [9] C. Donner, H. W. Jensen, "A spectral BSSRDF for shading human skin", *Proceedings of the 17th Eurographics Conference on Rendering Techniques*, 2006.
- [10] W. Jakob, Mitsuba renderer, <http://www.mitsubarenderer.org>, 2010.
- [11] H. W. Jensen, S. R. Marschner, M. Levoy, P. Hanrahan, "A Practical Model for Subsurface Light Transport", *Proceedings of the 28th annual conference on Computer graphics and interactive techniques*, p.511-518, 2001.